Lehikoinen, Antti; Chiodetto, Nicola; Arkkio, Antero; Belahcen, Anouar

**Improved sampling algorithm for stochastic modelling of random-wound electrical machines**

*Published in:*
The Journal of Engineering

*DOI:*
10.1049/joe.2018.8093

Published: 17/06/2019

*Document Version*
Publisher's PDF, also known as Version of record



*Please cite the original version:*
Lehikoinen, A., Chiodetto, N., Arkkio, A., & Belahcen, A. (2019). Improved sampling algorithm for stochastic modelling of random-wound electrical machines. *The Journal of Engineering*, (17), 3976-3980. https://doi.org/10.1049/joe.2018.8093

The Journal of Engineering

*The 9th International Conference on Power Electronics, Machines and Drives (PEMD 2018)*

# Improved sampling algorithm for stochastic modelling of random-wound electrical machines

eISSN 2051-3305
Received on 22nd June 2018
Accepted on 27th July 2018
E-First on 11th April 2019
doi: 10.1049/joe.2018.8093
www.ietdl.org

*Antti Lehikoinen[1] ✉, Nicola Chiodetto[2], Antero Arkkio[1], Anouar Belahcen[1]*
[1]*Department of Electrical Engineering and Automation, Aalto University, Espoo, Finland*
[2]*School of Electrical and Electronic Engineering, Newcastle University, Newcastle upon Tyne, England*
✉ *E-mail: antti.lehikoinen@aalto.fi*

**Abstract:** Random-wound electrical machines often suffer from high circulating current losses. These losses vary from machine to machine in a stochastic fashion. This study proposes an improved sampling algorithm for quantifying the uncertainty inherent in random windings. The algorithm is then combined with a circuit model to perform Monte Carlo analysis on the losses. The results are compared to measurements, and a good agreement is observed.

## 1 Introduction

Design of high-efficiency and high-performance electrical machine requires accurate prediction of resistive winding losses. These losses can be divided into skin- and proximity effects, and circulating currents. The latter can be especially significant and dominate in random-wound machines with stranded windings and a high-supply frequency, such as high-speed machines and multi-pole permanent magnet machines. Indeed, resistive loss increases of several tens of per cent have been observed [1, 2].

Due to manufacture reasons, the positions of the strands in a random-wound winding cannot be exactly known or controlled. In other words, their positions can be regarded as uncertain. Furthermore, they can vary significantly from slot to slot and machine to machine. Correspondingly, also the circulating current losses often exhibit significant variance, even between nominally identical machines [3]. As such, the losses are also stochastic in nature.

This paper extends the authors' previous work in [3] for uncertainty quantification of the circulating current losses. First, an equivalent circuit approach for modelling stranded windings is briefly recounted. Next, a phenomenological sampling algorithm is proposed for modelling the uncertainty in the winding. This algorithm is then coupled to the circuit model. Finally, the statistical properties of the resistive losses are then estimated with Monte Carlo analysis and compared to measurement data.

## 2 Modelling circulating currents

Some necessary basic theory is briefly presented here. First, the basics of the circulating current phenomenon are explained, followed by a light-weight circuit model suitable for their analysis. The circuit configuration is assumed fully know, i.e. the randomness is not taken into account until Section 3.

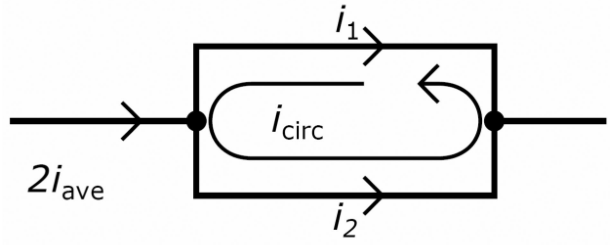


**Fig. 1** *Illustration of the circulating current phenomenon*

### 2.1 Circulating currents

Circulating currents can occur whenever two or more strands with different impedances are connected in parallel. The conductors draw different currents, which of course increases the total losses compared to an even distribution of current.

These currents can be decomposed to the average current component and a number of circulating current components. This gives the name to the phenomenon and has been illustrated for two conductors in Fig. 1. In the figure, the individual strand currents are denoted by $i_1$ and $i_2$. Correspondingly, the average current is $i_{\text{ave}}$, whereas $i_{\text{circ}}$ is the apparent circulating component.

It must be noted that differing impedances are not the only possible cause for circulating currents. Instead, they can also occur due to externally induced strand voltages, e.g. by permanent magnet flux partially penetrating into an open slot [4]. However, this paper focuses on solid-rotor induction machines, so this phenomenon is ignored. However, if needed, it can still be straightforwardly included in the circuit model described in the next section.

### 2.2 Circuit model

In random-wound induction machines, circulating currents are typically determined by the slot leakage inductances. Thus, they can be modelled by a circuit model as done by the authors in [3], based on the work of, e.g. van der Geest *et al*. [5] and Jiancheng *et al*. [6]. First, the strand voltages $\boldsymbol{u}_{\text{slot},k}$ in the slot $k$ are written as

$$\boldsymbol{u}_{\text{slot},k} = (\boldsymbol{R} + j\omega\boldsymbol{L}_\sigma)\boldsymbol{i}_{\text{strand},k} + \boldsymbol{e}_k, \quad (1)$$

where $\boldsymbol{i}_{\text{strand},k}$ denotes the strand currents, and $\boldsymbol{R}$ and $\boldsymbol{L}_\sigma$ are the strand resistance and leakage inductance matrices for the slot, respectively. The vector $\boldsymbol{e}_k$ denotes the strand voltages induced by the main flux, linking both the stator and the rotor, and will be discussed shortly.

Next, the strand currents are expressed with a set of linearly independent loop currents $\boldsymbol{i}$ as

$$\boldsymbol{i}_{\text{strand},k} = \boldsymbol{L}_k\boldsymbol{i}, \quad (2)$$

where $\boldsymbol{L}_k$ denotes the loop matrix for the slot $k$. Then, Kirchhoff's voltage law is applied to the strand voltages and the supply voltages $\boldsymbol{u}_\text{s}$:

$$\boldsymbol{u}_{\mathrm{s}} = \sum_{k=1}^{Q_{\mathrm{S}}} \boldsymbol{L}_k^T \boldsymbol{u}_{\mathrm{strand},k}, \tag{3}$$

where $Q_{\mathrm{s}}$ is the number of stator slots. Finally, (1)–(3) are combined, yielding the final system of equations

$$\boldsymbol{u}_{\mathrm{s}} = \sum_{k=1}^{Q_{\mathrm{S}}} \boldsymbol{L}_k^T(\boldsymbol{R} + \mathrm{j}\omega \boldsymbol{L}_\sigma)\boldsymbol{L}_k \boldsymbol{i} + \boldsymbol{L}_k^T e_k \,. \tag{4}$$

From this equation, the loop currents $\boldsymbol{i}$ can then be solved. The resistive losses in the strands can then be post-processed from the strand currents (2) and the strand resistances.

In an induction machine, the back-electromotive force vector $\boldsymbol{e}_k$ is strongly dependent on both the stator and rotor currents. Following the approach in [3], it can be written as

$$\boldsymbol{e}_k = \boldsymbol{K}_{s,k}\boldsymbol{i} + \boldsymbol{K}_{r,k} i_{\mathrm{r}} \tag{5}$$

where $i_{\mathrm{r}}$ is the rotor current space vector. The matrices $\boldsymbol{K}_{\mathrm{s},k}$ and $\boldsymbol{K}_{\mathrm{r},k}$ of rank 3 and rank 1, respectively, can be derived from the typical equivalent circuit parameters. Obviously, the system (4) has to be augmented by the rotor-branch voltage equation.

## 3 Stochastic modelling

In a random-wound machine, the positions of the individual strands inside slots cannot be accurately known or controlled. As the leakage inductances $\boldsymbol{L}_\sigma$ are strongly position dependent, the circulating current losses can vary considerably between nominally identical machines. Although long acknowledged, this stochastic behaviour has received relatively little attention in the literature [7].

### *3.1 Prior work*

In [8], the electric field in a random-wound transformer was briefly analysed. The analysis was based on first determining a set of possible strand positions, and then permuting the order of the strands within this set. This permutation could be decomposed into a set of pair-wise swapping of strand positions, which might be a clearer way to visualise the approach. This same approach was adopted and formally justified by Lehikoinen *et al*. [3].

This randomisation of the strand positions is equivalent to randomly permuting the rows of each of the loop matrices $\boldsymbol{L}_k$. The statistical behaviour can then be evaluated with, e.g. the Monte Carlo method. However, the problem of generating samples of suitably-distributed permutations still remains.

In [3], a rather complex sampling algorithm was proposed for generating permutations following a normal-like distribution, according to a special distance function. In addition, it was observed that the permutations for each slot could not be assumed statistically independent. Instead, a complex inter-slot dependency was defined to obtain satisfactory results. Thus, a special successive sampling scheme was developed, described next.

### *3.2 Proposed sampling algorithm*

Indeed, this paper proposes an improved, easier-to-implement sampling algorithm, also taking into account the apparent dependency between separate slots. The algorithm is based on a simplified model of the actual winding process. Specifically, it is assumed that each coil is first wound around a coil former outside the machine core. The coils would then be inserted into the slots through the slot openings. As the machines analysed later in this paper have semi-closed slots, this insertion has to be performed a few strands at a time.

Based on this process model, it can be assumed that any few strands that are close to each other in one slot are probably close to each other also in the next slot the coil passes through. Thus, the proposed algorithm can be summarised as follows.

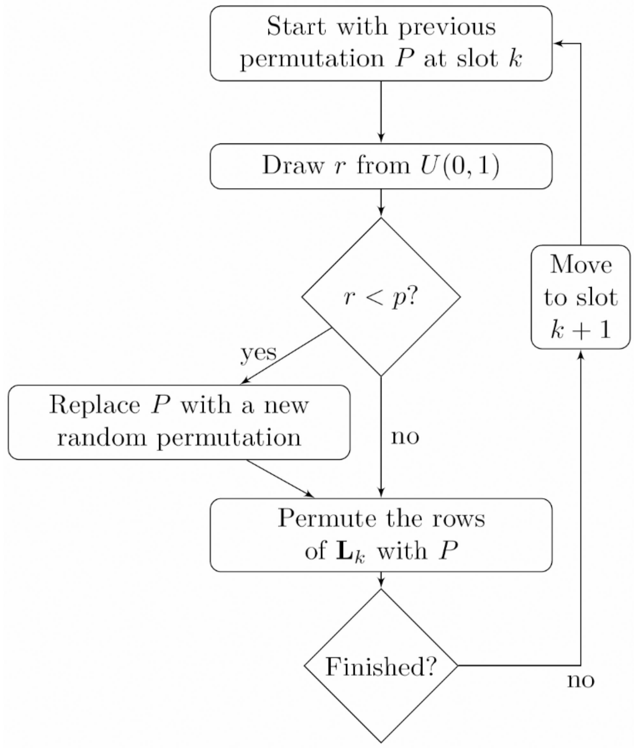


**Fig. 2** *Flowchart of the proposed algorithm*

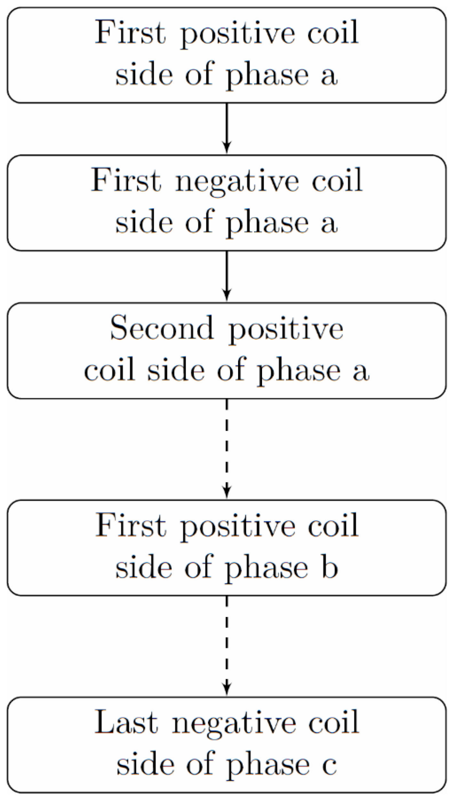


**Fig. 3** *Ordering of the coil sides used*

First, the parallel strands in a phase are divided into $n$ bundles. Then, between each two successive slots that the coil passes through, a random draw is made. With the probability $p$, the order of the bundles is changed according to a uniformly distributed random permutation. This permutation can be easily generated in most software environments, such as MATLAB or the NumPy package for Python. On the other hand, the order of the bundles is left intact with the probability $1-p$. The flow of the algorithm has been illustrated in Fig. 2, whereas Fig. 3 illustrates the order that the slots are traversed in.

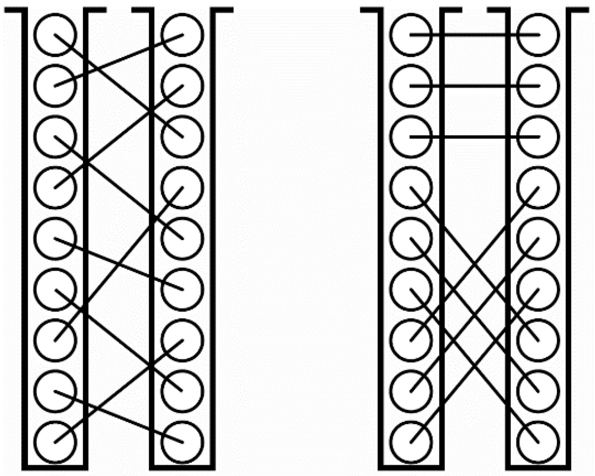

**Fig. 4** *Illustrative comparison of the old (left) and new (right) sampling algorithms for n = 3 bundles*

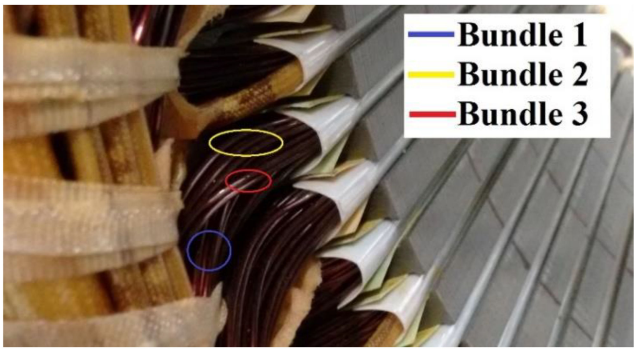


**Fig. 5** *Part of the end winding of a random-wound machine, with some spontaneously occurring strand bundles illustrated*

**Table 1** Machine characteristics

| Dimension | Value |
|---|---|
| stator diameter, mm | 290 |
| rated frequency, Hz | 450 |
| winding connection | delta |
| number of winding layers | 2 |
| number of turns | 3 |
| number of strands in a slot | 348 |
| number of stator slots | 36 |

An illustrative comparison between the old and the new sampling algorithms can then be found in Fig. 4, which visualises a randomisation of the strand order between two successive slots. As can be seen, with the old algorithm, the strands are crossing each other in an individual fashion. In reality, this would probably form a very messy-looking end-winding with fine braid-like structures. By contrast, with the new algorithm, the strands are moving in three larger bundles. Indeed, it could be argued that this is closer to the structure of an actual end-winding, such as the one illustrated in Fig. 5.

## 4 Simulation and measurement results

The proposed sampling algorithm was then used to analyse the circulating current losses and their variations in a high-speed induction motor with a rated power of roughly 200 kW. The main dimensions of the machines can be found in Table 1.

The results were then compared to the measurement data of 230 nominally identical motors. The circulating current factor

$$k_{\mathrm{cc}} = \frac{\sum_{k=1}^{N} |\boldsymbol{i}_k|^2}{(1/N)\left|\sum_{k=1}^{N} \boldsymbol{i}_k\right|^2} \tag{6}$$

was chosen as the quantity of interest. Here, $N$ denotes the number of parallel strands [1].

As a reference, Fig. 6 shows the estimated probability density distribution of $k_{\mathrm{cc}}$ at the rated frequency. Both the measured values and those simulated with the old sampling algorithm are shown. As can be seen, both distributions are roughly normal shaped and have similar mean values. However, the simulated values exhibit significantly smaller variance, resulting in a narrower distribution with a higher peak.

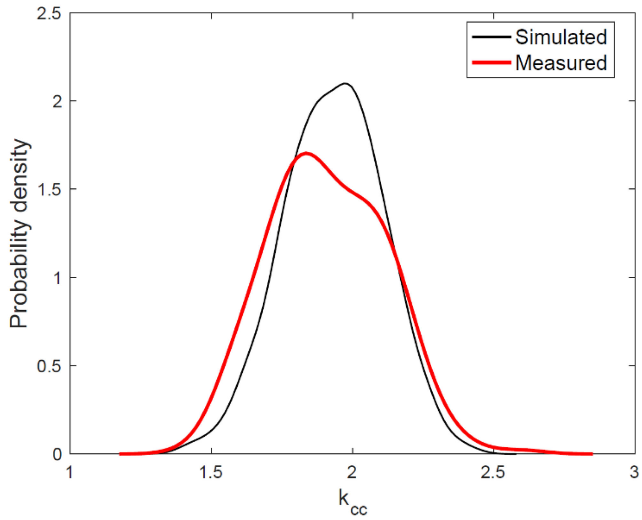


**Fig. 6** *Probability distribution of the circulating current factor at the rated frequency estimated from measurements, and simulated with the old sampling algorithm*

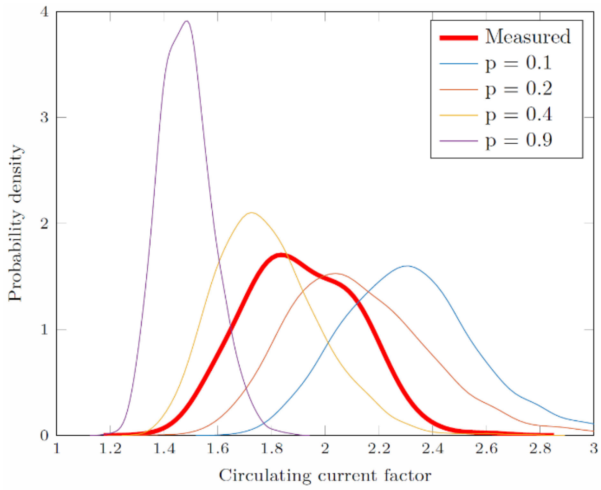


**Fig. 7** *Probability distributions obtained with different mixing probabilities, with n = 16*

### 4.1 Evaluation of the proposed algorithm

It must be stressed that the proposed new algorithm has two input arguments: the number of bundles $n$ and the mixing probability $p$. Hence, several Monte Carlo simulations were performed to evaluate their effect on the circulating current losses. The number of samples per simulation was set to 1000, as no significant differences could be seen in the results with larger sample sizes.

First, Fig. 7 shows the simulated probability density distributions of $k_{\mathrm{cc}}$ with different values of $p$. The number of bundles $n$ was kept constant at 16. As can be seen, the mixing probability has a relatively straightforward effect on the losses, with lower values of $p$ resulting in a wider distribution of $k_{\mathrm{cc}}$ with a larger mean. At first, this might seem paradoxical, with a less perturbed winding exhibiting higher losses. However, this well in line with the earlier observations [3].

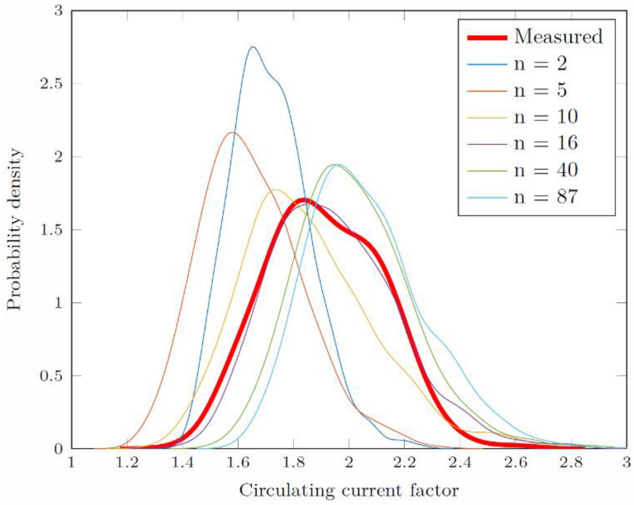


**Fig. 8** *Probability distributions obtained with different numbers of bundles, with p = 0.3*

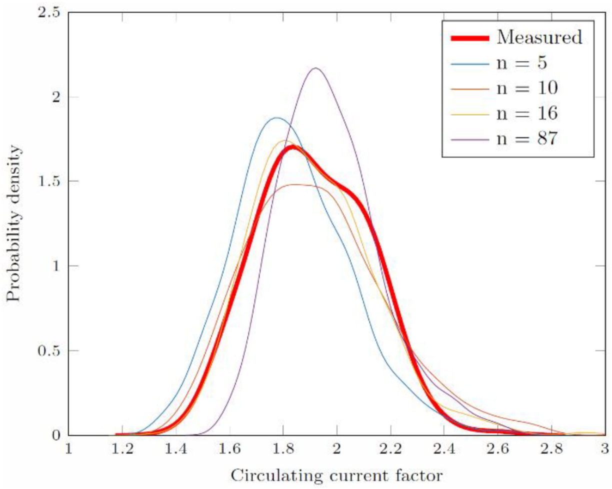


**Fig. 9** *Probability distributions (best fit) obtained with the new algorithm, with a different number of bundles n*

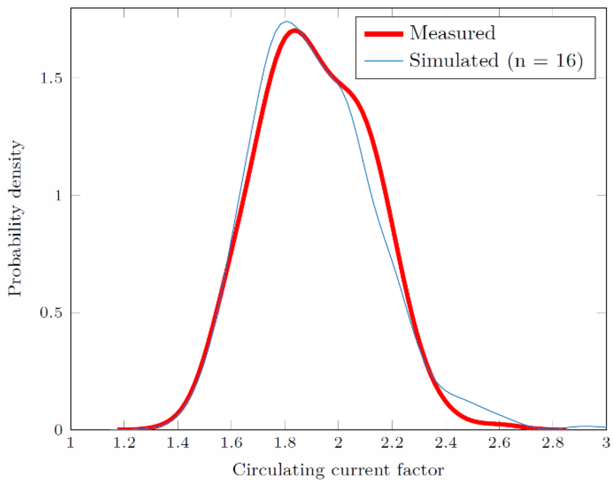


**Fig. 10** *Best-fitting results obtained with the new algorithm, with n = 16*

Next, the effect of the number of bundles $n$ was evaluated, with a constant $p = 0.3$. The results are again shown in Fig. 8. This time, a slightly more complex relationship can be established. With $n$ between 5 and 87, the mean value of $k_{cc}$ grows proportionally to $n$. However, the variance follows a parabolic dependence, obtaining its maximum at $n = 10$. Furthermore, both of these relationships break down at $n < 5$, as evident from the $n = 2$ curve. However, this case, i.e. having only two bundles, would represent a physically unrealistic situation anyway.

### 4.2 Performance evaluation

Next, the ability of the algorithm to match the measured results was evaluated. First, the number of bundles $n$ was varied between 5 and 87. Then, for each $n$, the mixing probability $p$ was adjusted to obtain the best possible agreement (in the mean-square sense) with the measurement data.

The results are shown in Fig. 9. As can be seen, even the worst-fitting results are on par with, or slightly better compared to the old algorithm of Fig. 6. Furthermore, it can be seen that the best results are indeed much better than previously.

This is further illustrated in Fig. 10, which shows the results obtained with $n = 16$. As can be seen, a very good agreement has been obtained with the measured results in general. Admittedly, the simulated distribution is slightly more right-tailed than the measured one, but this deviation is still relatively minor. Compared to the old algorithm of Fig. 6, a significant improvement can be seen. Furthermore, due to the understandably limited sample size of the measured data, it could be argued that the probability density estimated from the measurements is not very accurate. In other words, it cannot be confidently concluded which one of the presented curves is closer to the correct one.

### 4.3 Interpretation of the results

As was seen, the best results were obtained with 14–16 bundles. For the machine in question, this corresponds to a mean bundle size of 11–12 strands. Incidentally, this number is close to the size of the largest bundle that could fit through the slot opening during the winding process, namely 15 strands in a perfect circular packing. In other words, the simulation results seem to support the assumptions made in Section 3.2. about the winding process, i.e. assumption that the strands are inserted into the slots in the largest bundles fitting through the slot opening.

## 5 Conclusion

A sampling algorithm was proposed for modelling the uncertainty inherent in a random winding, and for quantifying the associated circulating current losses. The algorithm is simple to implement, and is based on a phenomenological model of the winding process. Properly tuned, the algorithm was able to closely match the probability distribution of measured losses in a series of high-speed induction machines.

The algorithm has two tuning parameters. However, based on the results presented, it seems that one of them – the number of bundles $n$ – can be estimated from the machine and winding dimensions. This would leave only the mixing probability $p$ to be estimated.

Obviously, some further work is still needed. So far, the algorithm has only been validated against one set of measurement data, so analysing additional machine types would be beneficial. However, this would probably require machine manufacturers to adopt circulating current measurements as a standard procedure.

## 6 Acknowledgments

The research leading to these results has received funding from the European Research Council under the European Union's Seventh Framework Programme (FP7/2007-2013)/ERC grant agreement no. 339380.

## 7 References

[1] Lähteenmäki, J.: 'Design and voltage supply of high-speed induction machines'. PhD Thesis, Helsinki University of Technology, Espoo, Finland, 2002

[2] Mellor, P., Wrobel, R., Salt, D., *et al.*: 'Experimental and analytical determination of proximity losses in a high-speed PM machine'. IEEE Energy Conversion Congress and Exposition, Denver, CO, USA, September 2013, pp. 3504–3511

[3] Lehikoinen, A., Chiodetto, N., Lantto, E., *et al.*: 'Monte Carlo analysis of circulating currents in random-wound electrical machines', *IEEE Trans. Magn.*, 2016, **52**, (8), pp. 1–12

[4] Tessarolo, A., Agnolet, F., Luise, F., *et al.*: 'Use of time-harmonic finite-element analysis to compute stator winding eddy-current losses due to rotor motion in surface permanent-magnet machines', *IEEE Trans. Energy Convers.*, 2012, **27**, (3), pp. 670–679

[5] van der Geest, M., Polinder, H., Ferreira, J.A., *et al.*: 'Current sharing analysis of parallel strands in low-voltage high-speed machines', *IEEE Trans. Ind. Electron.*, 2014, **61**, (6), pp. 3064–3070

[6] Jiancheng, F., Xiquan, L., Han, B., *et al.*: 'Analysis of circulating current loss for high-speed permanent magnet motor', *IEEE Trans. Magn.*, 2015, **51**, (1), pp. 1–13

[7] Mesrobian, A., Holdrege, J.H.: 'Random wound versus form wound on low voltage synchronous generators'. 37th Annual Conf. on Petroleum and Chemical Industry, Houston, TX, USA, 1990, pp. 185–190

[8] Canali, A., Mazauric, V., Leconte, V., *et al.*: 'Modeling of a random distribution of turns in wrapped windings'. 12th Biennial IEEE Conf. on Electromagnetic Field Computation, Miami, FL, USA, 2006, pp. 361–361